Anomeric Effect in Furanosides. Experimental Evidence from Conformationally Restricted Compounds

Ulf Ellervik and Göran Magnusson*

Contribution from the Department of Organic Chemistry 2, Chemical Center, The Lund Institute of Technology, University of Lund, P.O. Box 124, S-221 00 Lund, Sweden

Received October 21, 1993®

Abstract: A series of conformationally restricted *O*-, *C*-, *S*-, and *N*-"furanosides" have been synthesized, where the number 3 and 4 carbons are part of a norbornane ring system. All the carbons of the tetrahydrofuran ring are kept in one plane by the rigid norbornane skeleton, permitting only the ring oxygen to move above or below the tetrahydrofuran ring plane. This causes the substituents on carbon 2 to occupy a pseudoaxial or a pseudoequatorial position. The "norbornane–furanosides" were investigated by NMR, X-ray crystallography, and molecular mechanics calculations. The *O*- and *S*-furanosides preferred the conformation with a pseudoaxial anomeric substituent, whereas its *C*-furanosidic counterpart preferred the conformation with a pseudoequatorial substituent. These findings constitute the first demonstration of a "by definition" anomeric effect in furanosides.

The tendency of electronegative substituents at C-1 of pyranose derivatives to occupy preferentially an axial position is termed the anomeric effect.[1,2] In addition to the numerous examples from carbohydrate pyranose chemistry, the anomeric effect has been observed in a number of other structural types and many reviews have summarized the phenomenon.[3] Its origin may be found in destabilization of equatorial substituents due to unfavorable dipole–dipole interactions (Figure 1). An alternative view is stabilization due to favorable overlap between the orbital carrying a ring-oxygen lone pair of electrons and the σ^* orbital of the bond between C-1 and the electronegative substituent. A hyperconjugative effect has also been suggested, which would explain the slightly altered bond lengths to the anomeric carbon in pyranosides. Since C-1 carries two oxygen atoms, an exo-anomeric effect[4] has been suggested on the basis of the same kind of reasoning as above. However, purely steric arguments[5] point in the same direction and it is at present an open question which of the "stereoelectronic" and the "steric" views that is the most correct one. The different interpretations of the anomeric effect are depicted in Figure 1.

Furanosides have received much less attention than pyranosides regarding the anomeric effect. This is probably due to the fact that the different conformations of five-membered rings have quite similar energies,[6] whereas six-membered rings are normally present in a single low-energy chair conformation. Therefore, axial and equatorial substituents in pyranosides are easily identified (e.g., by NMR techniques), in contrast to the case with furanosides.

A limited number of reports on an anomeric effect in furanosides have appeared in the literature. In the crystal state, furanoside structures stored in the Cambridge Crystallographic Data Base had the anomeric alkoxy substituent in a pseudoaxial (pax) orientation, in contrast to cyclopentanes, where alkoxy substituents showed a slight preference for the pseudoequatorial (peq) arrangement.[7] Similar results were obtained with a number of methyl 3,6-anhydrohexofuranosides[8] and nucleosides.[9]

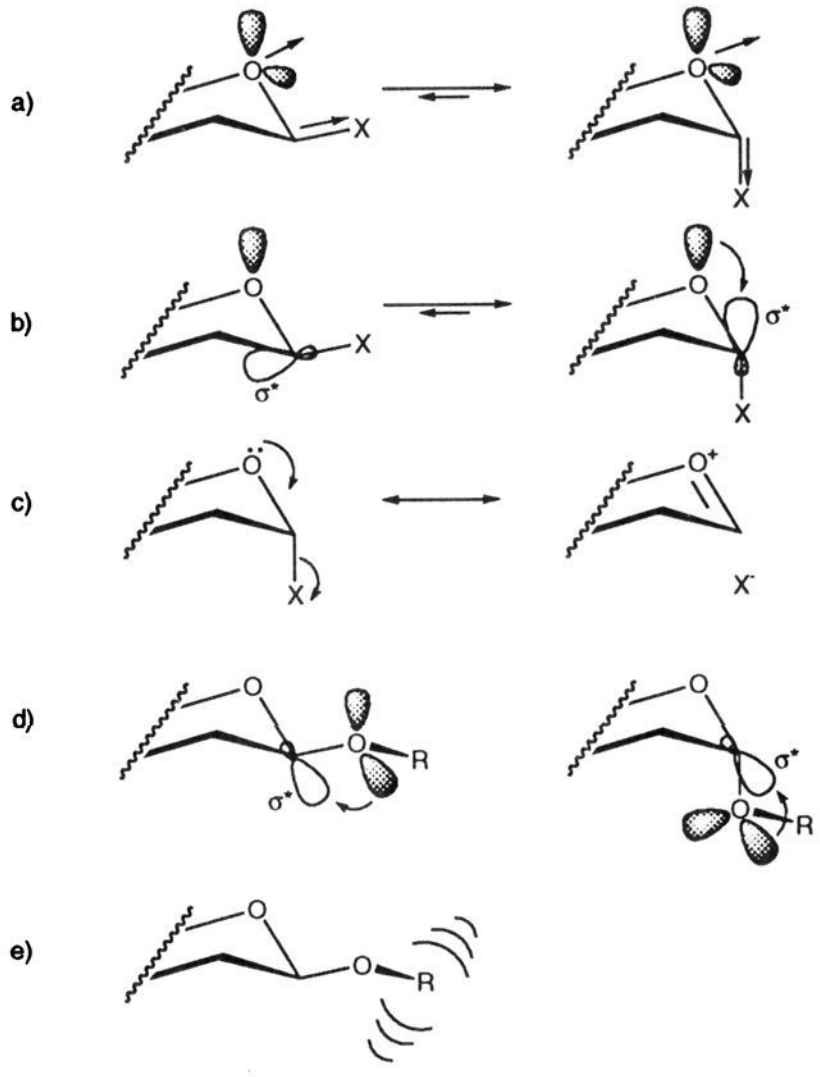

Figure 1. The anomeric effect, described by (a) unfavorable dipole–dipole interaction with equatorial substituents; (b) favorable overlap between filled ring-oxygen lone pair orbitals and an empty σ^* orbital; (c) hyperconjugation in axially substituted compounds; (d) exo-anomeric effect in β and α glycosides; (e) exo-anomeric effect due to steric interactions.

We realized that conformationally restricted furanosides, where all ring carbons are kept in one plane, would allow only two envelope conformations, with the ring oxygen positioned either above or below the ring-carbon plane. In a conformational equilibrium, an anomeric substituent would thus occupy either

* Corresponding author.

• Abstract published in *Advance ACS Abstracts,* February 1, 1994.

(1) Edward, J. T. *Chem. Ind.* (*London*) **1955**, 1102.
(2) Lemieux, R. U. Explorations with Sugars–How Sweet It Was. In *Profiles, Pathways and Dreams*; Seeman, J. I., Ed.; American Chemical Society: Washington, DC, 1990.
(3) Juaristi, E.; Cuevas, C. *Tetrahedron* **1992**, *48*, 5019.
(4) Praly, J.-P.; Lemieux, R. U. *Can. J. Chem.* **1987**, *65*, 213.
(5) Goekjian, P. G.; Wu, T.-C.; Kishi, Y. *J. Org. Chem.* **1991**, *56*, 6412.
(6) Angyal, S. J. *Adv. Carbohydr. Chem. Biochem.* **1984**, *42*, 15.
(7) (a) Cossé-Barbi, A.; Dubois, J. E. *J. Am. Chem. Soc.* **1987**, *109*, 1503. (b) Cossé-Barbi, A.; Watson, D. G.; Dubois, J. E. *Tetrahedron Lett.* **1989**, *30*, 163.
(8) Kopf, J.; Köll, P. *Carbohydr. Res.* **1984**, *135*, 29.
(9) Koole, L. H.; Buck, H. M.; Nyilas, A.; Chattopadhyaya, J. *Can. J. Chem.* **1987**, *65*, 2089.

0002-7863/94/1516-2340$04.50/0

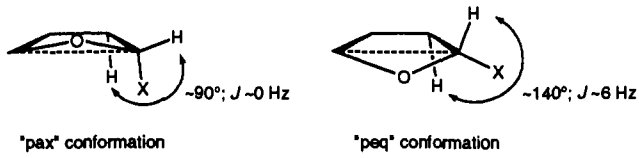

Figure 2. The electronegative substituent X occupies either a pseudoaxial (pax) or a pseudoequatorial (peq) position in a conformationally restricted furanose molecule, where the ring carbons are locked in a planar arrangement. The preferential conformation can be determined from the anomeric proton coupling constant *J*.

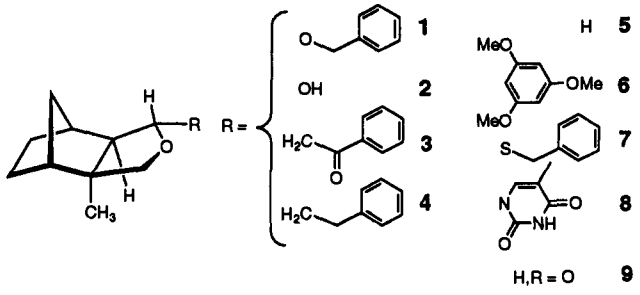

Figure 3. Norbornyl tetrahydrofuran derivatives used in this study.

a pseudoaxial or a pseudoequatorial position, which can be identified by the coupling constant of the anomeric hydrogen as illustrated in Figure 2. It should be noted that this type of limited conformational equilibrium in a furanoside is principally similar to the axial ↔ equatorial equilibrium of the anomeric substituent in the two chair forms of a pyranoside. We also realized that a demonstrated conformational difference between an *O*-furanoside and the corresponding *C*-furanoside would constitute a "by definition" demonstration of an anomeric effect in these compounds.

We have chosen norbornyl furanosides (Figure 3) for our study since the norbornane skeleton is highly rigid and should therefore keep the furanoside ring carbons in one plane, allowing only the ring oxygen to move above or below the plane. The two conformations possible for the benzyl furanoside **1** are shown as a stereorepresentation in Figure 4. The pseudoaxial ↔ pseudoequatorial equilibria were investigated by various NMR methods, X-ray crystallograpy (with **6**), and molecular mechanics (MM2) calculations. The conclusion is that furanosides display an anomeric effect. For example, in the case of the *O*-furanoside **1**, the pseudoaxial conformation is favored by ~10 kJ/mol according to the MM2 calculations. This is in full accord with the NMR results as discussed below.

Synthesis of Compounds 1–13

Compound **10** was synthesized as described[10] and hydrogenated to give **11** (67%), which in turn was reduced with hydrazine hydrate[11] to give **1** (87%). During the latter step, it was important to remove water in order to avoid formation of the corresponding primary alcohol by incomplete reduction. Compound **1** was used as the starting material for the synthesis of compounds **2–13**, as depicted in Scheme 1.

Hydrogenolysis of **1** gave the hemiacetal **2** (88%) and its anomer in a diastereomeric ratio of 97:3. Column chromatography of the mixture gave pure **2**. The hydrogenolysis reaction was somewhat unpredictable, sometimes leading to cleavage between oxygen and the tetrahydrofuran ring (→ **5**).

Treatment of **1** with α-((trimethylsilyl)oxy)styrene and boron trifluoride etherate gave ketone **3** (93%), which was reduced with hydrazine hydrate[11] to give **4** (51%), which is the *C*-furanoside analog of **1**.

(10) Rehnberg, N.; Sundin, A.; Magnusson, G. *J. Org. Chem.* **1990**, *55*, 5477.
(11) Huang-Minlon *J. Am. Chem. Soc.* **1949**, *71*, 3301.

Compound **2** was reduced with lithium aluminium hydride to give the diol **12** (92%), and treatment of **12** with triphenylphosphine–diethyl azodicarboxylate[12] in deuteriochloroform gave the tetrahydrofuran derivative **5**. Purification of **5** was complicated by its high volatility. Therefore, the crude material was extracted with ether and the solvent was removed by column distillation. The residue was chromatographed with an ether–pentane mixture, deuteriochloroform was added, and ether and pentane were removed by column distillation. The addition of deuteriochloroform and distillation were repeated twice, thus furnishing a solution of **5** in deuteriochloroform suitable for NMR investigation. The yield of **5** was not determined by isolation but could be estimated to be ~90%.

Oxidation of **2** with chromium trioxide in pyridine gave the lactone **9** (70%).

Treatment of compound **1** with 1,3,5-trimethoxybenzene and boron trifluoride etherate gave the aromatic *C*-furanoside **6** (93%) as a crystalline solid.

Treatment of compound **1** with benzyl thioalcohol and boron trifluoride etherate gave the *S*-furanoside **7** (97%).

Treatment of **7** with bis(trimethylsilyl)thymine and *N*-bromosuccinimide[13] gave a mixture of the *N*-glycosides **8** and **13** in 90% yield. The mixture was partially separated by chromatography to give NMR samples of pure **8** and **13**.

Structure Determination of Compounds 1–13

The structures of **1–13** were determined by analysis of their NMR spectra (Table 1), including COSY, NOESY, and differential NOE measurements. In addition, the structure of **6** was confirmed by X-ray crystallography[14] as shown below. The hydrogen-atom numbering used in the figures and tables is depicted in Figure 5. All NMR data are fully consistent with the proposed structures, and the synthetic steps used are not supposed to cause any rearrangements or other undesired reactions. Accordingly, the norbornane/tetrahydrofuran ring system is conserved in all the compounds (except **12**), leaving only the crucial anomeric configuration undetermined in compounds **2–4** and **6–8**.

Compound **1** was synthesized from the known[10] aldehyde **10** and used as starting material for the synthesis of **2–9**. Since the present investigation is based on **1–9**, a correct structure for **1** is a necessary foundation for the discussion below of the anomeric effect. The anomeric hydrogen signal at 4.86 ppm is a sharp singlet. Only the configuration having H_5 and H_6 in a *trans* relationship allows a H_5–H_6 angle close to 90°, as required by the Karplus curves.[15] Irradiation of H_5 and H_{3a} gave NOE's at H_{10a}, thereby confirming the anomeric configuration of **1**. COSY and NOESY experiments permitted full assignment of the remaining hydrogens; chemical shifts and coupling constants are shown in Table 1.

The ^{1}H-NMR spectrum of compound **2** was very similar to that of **1**, the main difference being the presence of a hydroxylic hydrogen doublet at 2.30 ppm and a H_5 doublet due to coupling to the hydroxylic hydrogen. Addition of D_2O caused the H_5 doublet to collapse to a sharp singlet.

The H_5 hydrogen of compound **3** couples to H_6 and the "anomeric" methylene group with the same coupling constants ($J \sim 6.3$ Hz), and therefore the H_5 signal occurs as a quartet (at 4.07 ppm). Irradiation of H_5 and H_{3a} gave NOE's at H_{3a}, H_{10a} and H_5, H_{10a}, respectively (Table 2), thereby confirming the "anomeric" configuration.

The H_5 signal of compound **4** was partly obscured by that of H_{3a}. However, saturation of the H_{3b} signal caused the H_{3a} signal

(12) Mitsunobu, O. *Synthesis* **1981**, 1.
(13) Sujino, K.; Sugimura, H. *Synlett.* **1992**, 553.
(14) Richardson, J. F. University of Louisville, personal communication.
(15) Jackman, L. M.; Sternhell, S. *Applications of Nuclear Magnetic Resonance Spectroscopy in Organic Chemistry*, 2nd ed.; Pergamon Press: Braunschweig, 1969.

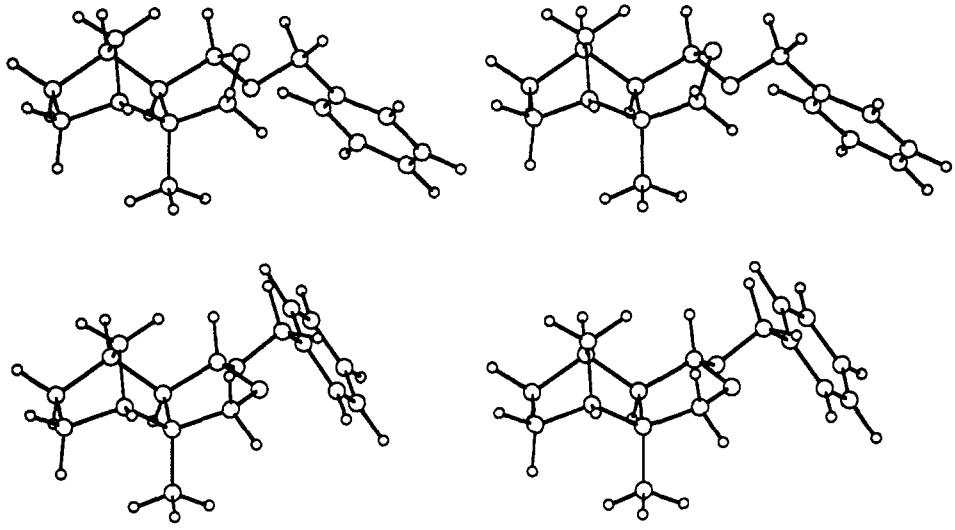

Figure 4. Stereostructures showing the $\mathbf{1}_{pax}$ and $\mathbf{1}_{peq}$ minimum energy conformations, calculated by the MM2(91) force field.[16,17,20]

Scheme 1[a]

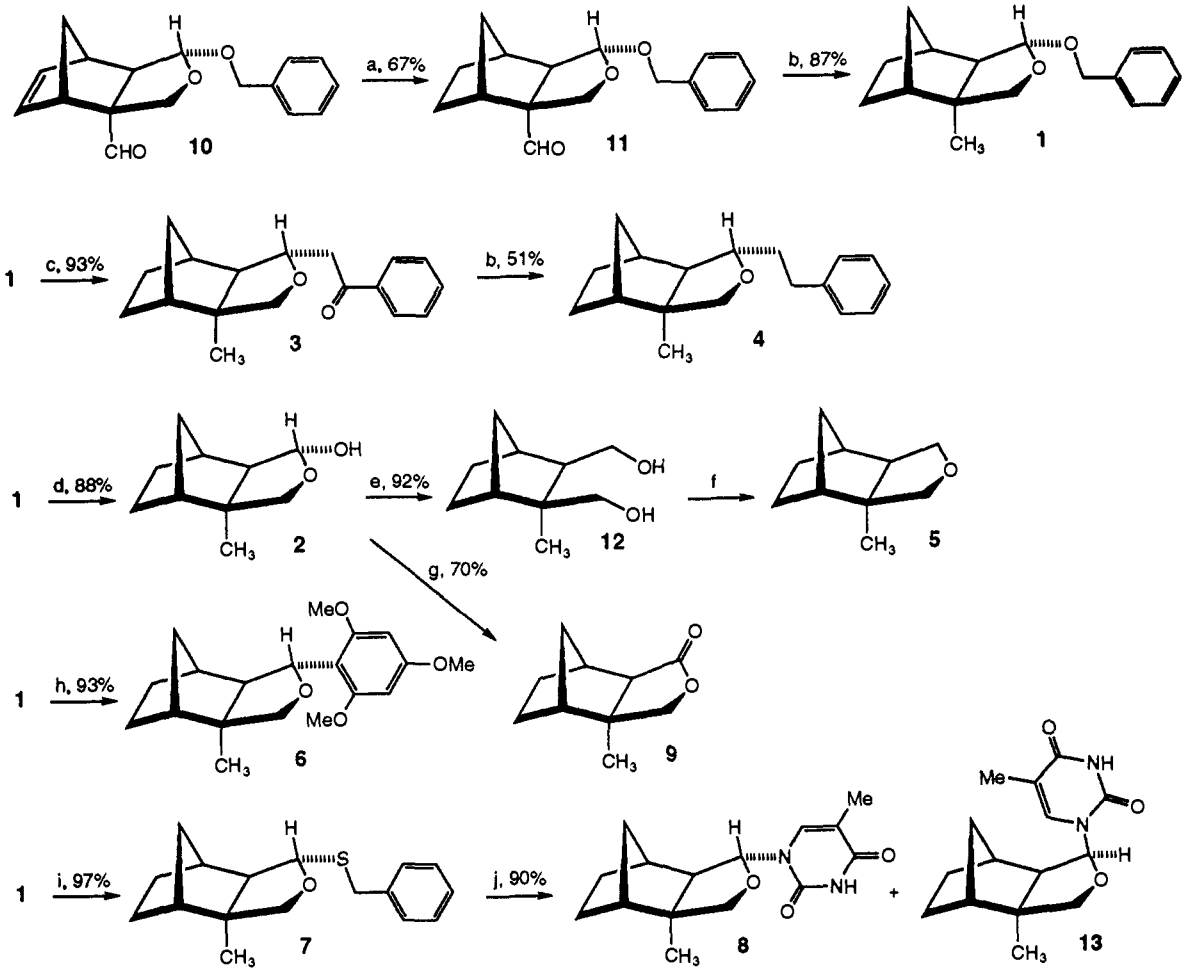

[a] (a) H_2, Pd/C, NaOMe/MeOH. (b) KOH, $H_2NNH_2 \cdot H_2O$, $HOCH_2CH_2OH$, 130–200 °C. (c) 1-Phenyl-2-((trimethylsilyl)oxy)ethylene, BF_3Et_2O, CH_2Cl_2. (d) H_2, Pd/C, THF. (e) $LiAlH_4$, Et_2O. (f) Ph_3P, DEAD, $CDCl_3$. (g) CrO_3, pyridine, CH_2Cl_2. (h) 1,3,5-Trimethoxybenzene, BF_3Et_2O, CH_2Cl_2. (i) Benzyl mercaptan, BF_3Et_2O, CH_2Cl_2. (j) Thymine, $(Me_3Si)_2NH$, Me_3SiCl, DMF, CH_2Cl_2, then added to **7**, molecular sieve, NBS, –70 °C, CH_2Cl_2.

to collapse into a singlet, thereby permitting an analysis of the H_5 doublet of triplet pattern (J = 7.9, 5.3 Hz). Saturation of the "anomeric" methylene group caused H_5 to collapse into a doublet with $J \sim 7.9$ Hz.

The H_5 signal of compound **6** is a doublet with J = 7.6 Hz. Irradiation of H_5 and H_{3a} gave NOE's at H_{3a}, H_{10a} and H_5, H_{10a}, respectively (Table 2), thereby confirming the "anomeric" configuration. It was corroborated by the single-crystal X-ray structure of **6** (Figure 6).[14]

The spectrum of the "thioglycoside" **7** was very similar to that of **1**; only the expected small chemical shift differences were observed. Irradiation of H_5 and H_{3a} gave NOE's at H_{10a} (Table 2), thereby confirming the "anomeric" configuration.

The H_5 signal of compound **8** is a doublet with J = 4.0 Hz.

Table 1. ^{1}H-NMR Chemical Shifts (δ) and Coupling Constants (J) for Compounds 1–13

compound		H-1	H-3	H-5	H-6	H-7	H-8	H-9	H-10a	H-10b	H-11	H-12	CH_3
1	δ	1.91	3.76, 3.69	4.86	1.63	2.11	1.55–1.60, 1.10–1.15	1.50–1.55, 1.25–1.30	1.83	1.05		4.67, 4.41	1.20
	J	d, 3.5	ABq, 8.5	s	d, 1.4	d, 3.9	m	m	dt, 10.0, 1.9	dq, 10.0, 1.5		ABq, 12.0	s
2	δ	1.91	3.88, 3.68	5.18	1.55	2.14	1.45–1.65, 1.10–1.30	1.45–1.65, 1.25–1.35	1.78	1.07			1.22
	J	d, 3.5	ABq, 8.7	d, 2.3	s	d, 4.0	m	m	dt, 10.2, 1.8	dd, 11.2, 1.5			s
3	δ	1.93	3.64, 3.50	4.07	1.23	2.20	1.55–1.60, 1.05–1.10	1.50–1.55, 1.30–1.35	1.83	1.12	3.41, 3.08		1.13
	J	d, 3.8	ABq, 8.8	q, 6.3	dd, 6.0, 1.8	d, 4.6	m	m	dp, 10.4, 2.0	dq, 10.4, 1.6	dABq, 15.9, 6.7		s
4	δ	1.90–1.95	3.86, 3.47	3.44	1.90–1.95	2.02	1.50–1.60, 1.15–1.25	1.50–1.60, 1.30–1.40	1.80	1.11	1.80–1.90,	2.76, 2.65	1.14
	J	m	ABq, 8.7	dt, 7.9, 5.3	m	d, 4.3	m	m	d, 10.7	dd, 10.3, 1.6	m, 1.90–2.00	ddABq, 13.9, 10.5, 5.7	s
5	δ	1.92	3.49	3.94, 3.42	1.45–1.55	1.98	1.45–1.60, 1.00–1.10	1.45–1.60, 1.20–1.30	1.82	1.05			1.09
	J	d, 3.8	d, 2.1	dd, 9.1, 7.4 dd, 9.1, 4.8	m	d, 4.7	m	m	dp, 9.9, 2.0	dq, 10.2, 1.7			s
6	δ	1.95–2.00	3.76, 3.53	4.96	1.87	2.02	1.50–1.60, 1.00–1.10	1.50–1.60, 1.30–1.40	1.95–2.00	1.13			1.27
	J	m	ABq, 8.6	d, 7.6	dd, 7.5, 1.7	d, 4.7	m	m	m	dd, 10.7, 1.6			s
7	δ	1.95	3.91, 3.68	4.96	1.43	2.07	1.45–1.50, 1.15–1.20	1.55–1.60, 1.25–1.30	1.87	1.07		3.81, 3.67	1.20
	J	d, 4.7	ABq, 9.0	d, 1.4	s	d, 4.6	m	m	dp, 10.0, 2.3	dq, 8.6, 1.5		ABq, 13.5	s
8	δ	1.99	3.90, 3.73	5.66	1.52	2.43	1.60–1.65, 1.10–1.15	1.55–1.60, 1.35–1.40	1.73	1.26	7.13	1.94	1.22
	J	d, 3.4	ABq, 9.0	d, 4.0	dd, 3.9, 1.8	d, 4.6	m	m	d, 10.7	dd, 10.6, 1.5	q, 1.2	d, 1.2	s
9	δ	2.05	4.05, 3.97		1.93	2.58	1.63–1.68, 1.20–1.25	1.55–1.59, 1.35–1.41	1.51	1.31			1.19
	J	d, 2.8	ABq, 9.3		d, 2.2	d, 4.5	m	m	d, 9.3	dd, 10.8, 1.4			s
10	δ	2.93	4.37, 3.72	5.00	2.43	2.93	6.31	6.26	1.99	1.41		4.70, 4.46	
	J	s	d, 9.6	s	d, 1.6	s	dd, 5.3, 3.0	dd 5.3, 3.0	d, 9.1	dd, 9.1, 1.5		ABq, 12.0	
11	δ	2.30	4.14, 3.72	4.97	2.44	2.46	1.2–1.7	1.2–1.7	1.89	1.18		4.65, 4.42	
	J	d, 3.0	ABq, 9.5	s	d, 0.9	d, 3.8	m	m	dt, 10.9, 1.7	d, 10.6		ABq, 12.0	
12	δ	1.71	3.92, 3.69	3.60, 3.34	1.7–1.8	1.91	1.2–1.5	1.2–1.5	1.57	1.12			1.15
	J	d, 2.4	ABq, 11.0	dd, 11.5, 4.3 d, 11.1	m	d, 4.8	m	m	dt, 8.5, 2.2	dd, 10.3, 1.6			s
13	δ	2.07	3.92, 3.72	5.79	1.98	1.86	1.55–1.60, 1.10–1.15	1.50–1.55, 1.30–1.40	1.62	1.12	7.41	1.93	1.21
	J	d, 3.0	ABq, 9.2	d, 6.1	dd, 6.1, 1.6	d, 4.4	m	m	d, 10.0	dd, 10.1, 1.4	d, 1.2	d, 1.2	s

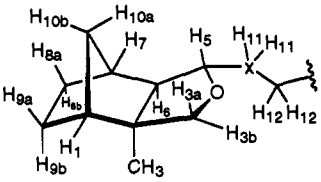

Figure 5. The numbering system used for compounds **1–13**.

Table 2. Nuclear Overhauser Enhancements (%) for Compounds **1**, **3**, **6**, **7**, and **8**

		H_{obsd}[b]					
compd	H_{irr}[a]	H_1	H_{3a}	H_5	H_6	H_7	H_{10a}
1	H_{3a}	6.9		0.1			2.8
	H_5		0.6		2.8	6.5	2.3
3	H_{3a}	5.5		2.7			4.8
	H_5		1.8		1.3	3.9	5.7
6	H_{3a}	3.8		2.8			4.1
	H_5		1.9		1.3	3.5	5.6
7	H_{3a}	4.1		0.7			1.5
	H_5		0.9		2.7	5.8	2.1
8	H_{3a}	3.3		1.8			3.6
	H_5		1.2		1.3	3.0	4.1

[a] Irradiated hydrogen. [b] Observed hydrogen.

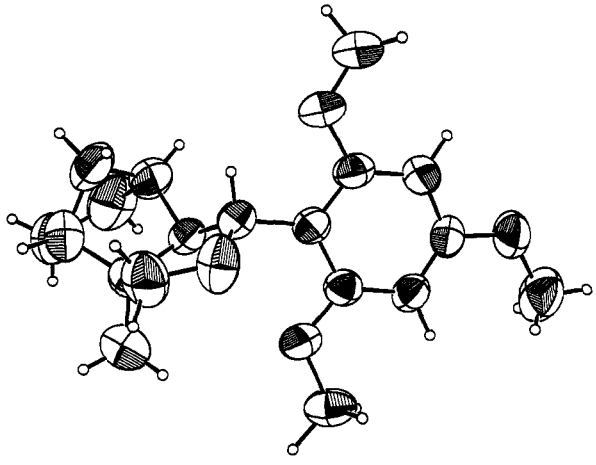

Figure 6. ORTEP drawing of the crystal structure of **6**.

Irradiation of H_5 gave an NOE at H_{10a}. There is also a weak NOE between H_5 and H_{3a}. Compound **13** had an NOE between H_5 and H_{3b}, and between H_{3b} and CH_3, which confirmed the structural assignments for both **8** and **13**.

With the structures of compounds **1–8** in hand, careful dissection of the NMR and X-ray data was made and the results were supported by MM2 calculations. The minimum energy conformations of **1–6** were determined by molecular mechanics calculations, using the MM2(91) force field.[16,17] The dihedral driver option (10° increment in the O_4–C_5–X–C_{12} (Ψ) angle) in the MacMimic/MM2(91) software package[17] allowed determination of the probable global energy minimum for each of the compounds **1–4** and **6**. Selected torsional angles and interatomic distances for the pax and peq conformations are given in Table 3, and the minimum energies are given in Table 4.

Discussion

The most significant result of this investigation is the reversed conformational preference of the *O*- and *C*-furanosides **1** and **4** (Table 4). The *O*-furanoside prefers the $\mathbf{1}_{pax}$ over the $\mathbf{1}_{peq}$ conformation by ~10 kJ/mol according to the MM2 calculations. This gives a Boltzman distribution of ~99:1, meaning that the H_5–C_5–C_6–H_6 torsional angle (93°) of $\mathbf{1}_{pax}$ dominates the magnitude of the $H_{5,6}$ coupling constant ($J \sim 0$ Hz). The Karplus curves predict a value of ~0 Hz, which is in agreement with the measured value. Furthermore, in a previous paper,[10] it was shown that, in all compounds with a H_5–H_6 *trans* arrangement (10 norbornene furanosides), the H_5 signal was a singlet, which corroborates the findings above. The corresponding *C*-furanoside prefers $\mathbf{4}_{peq}$ over $\mathbf{4}_{pax}$ by 4.5 kJ/mol, according to MM2 calculations. This preference is reflected in the coupling constant (J = 7.9 Hz) found for compound **4** (Table 4). Similar conformational preferences were observed for the hemiacetal **2** (pax conformation), the *S*-furanoside **7**, and the *C*-furanosides **3** and **6** (peq conformation). The preferred $\mathbf{6}_{peq}$ conformation was deduced from the $H_{5,6}$ coupling constant (J = 7.6 Hz) and corroborated by the X-ray structure as shown in Figure 6 and Tables 3 and 4. The similarity between the X-ray and calculated structures for **6** is depicted in Figure 7.

It should be noted that the C_6–C_5–X–C_{12} torsional angles of the calculated minimum energy conformations of $\mathbf{1}_{pax}$ and $\mathbf{4}_{pax}$, as well as $\mathbf{1}_{peq}$ and $\mathbf{4}_{peq}$, are quite similar (Table 3 and Figure 8). As with *O*- and *C*-pyranosides,[5] the conformational preference of the aglycon in **1** and **4** seems to be governed more by a steric than by an electronic exo-anomeric effect.

The conformational energy difference for **5** is small (0.6 kJ/mol; Table 4), which shows that there is no large intrinsic conformational preference in the basic ring system of the compounds investigated here. The small energy difference is corroborated by the intermediate sized $H_{5,6}$ coupling constant (J = 4.8 Hz). Therefore, the conformational preferences of **1–4** and **6–8** must mainly emanate from the substituents present at C_5.

The NMR spectrum (Table 1) of the *S*-glycoside **7** was similar to that of **1**. The H_5 signal for **7** was a doublet with a small coupling constant (1.4 Hz), indicating that **7** had a somewhat smaller pax/peq ratio than **1**. The *N*-glycoside **8** had a $H_{5,6}$ coupling constant of 4.0 Hz, which is consistent with a rather small anomeric effect.

The NOE effects shown in Table 2 are fully consistent with the conformations proposed by analysis of the coupling constants. Thus, irradiation of H_{3a} (or H_5) gave a rather weak NOE on H_5 (or H_{3a}) in compounds **1** and **7** (where H_{3a} and H_5 are far apart due to pseudoequatorial orientations), whereas the effect was substantially stronger in the *C*-furanosides **3** and **6** (where H_{3a} and H_5 are closer in space due to the pseudoaxial orientations). In the *N*-furanoside **8**, the effect was intermediate. Irradiation of H_5 gave a strong NOE on H_6 in compounds **1** and **7** and a weak NOE in compounds **3** and **6**, as expected from the H_5–C_5–C_6–H_6 torsional angles and corresponding H_5–H_6 distance. Similarly, irradiation of H_5 and H_{3a} gave relatively weak NOE's on H_{10a} in **1** and **7** and strong NOE's in **3** and **6**, as expected from the interatomic distances.

The rather large difference in chemical shift between H_{10a} and H_{10b} in compounds **1–11** is probably due to deshielding of H_{10a} and thereby shielding of H_{10b} by the furanose ring oxygen O_4. It seems as if O_4 pushes electrons from the C_{10}–H_{10a} bond into the C_{10}–H_{10b} bond, thereby causing shielding of the latter two atoms; the ^{13}C signal for C_{10} was shifted upfield ~7 ppm in norbornanes having an exo-furanose ring, as compared to those having an endo-furanose ring.[10] It has been suggested[18,19] that deshielding of hydrogen by oxygen requires that the oxygen and hydrogen atoms are in repulsive van der Waals contact, i.e. at an interatomic distance of <2.7 Å. This is fulfilled for the pax but not for the peq conformations (Table 3). The O_4–H_{10a} distance for the peq conformations exceeds 3.2 Å. In the lactone **9**, the O_4–H_{10a}

(16) Burkert, U.; Allinger, N. L. *Molecular Mechanics*; American Chemical Society: Washington, DC, 1982.
(17) Molecular construction and energy minimization were made with the MacMimic/MM2(91) package: InStar Software, Ideon Research Park, S-223 70 Lund, Sweden.
(18) Thögersen, H.; Lemieux, R. U.; Bock, K.; Meyer, B. *Can. J. Chem.* **1982**, *60*, 44.
(19) Bock, K.; Frejd, T.; Kihlberg, J.; Magnusson, G. *Carbohydr. Res.* **1988**, *176*, 253.

Table 3. Torsional Angles and Interatomic Distances for Compounds **1–6**

compd	method[a]	torsional angle (deg)				distance (Å)		
		O_4–C_5–C_6–C_7	H_5–C_5–C_6–H_6	O_4–C_5–X–C_{12}	C_6–C_5–X–C_{12}	O_4–C_5	O_4–H_{10a}	H_5–H_{10a}
$\mathbf{1}_{pax}$	MM2(91)	89	93	75	170	1.406	2.482	3.005
$\mathbf{1}_{peq}$	MM2(91)	130	136	75	170	1.418	3.270	2.367
$\mathbf{2}_{pax}$	MM2(91)	91	92			1.390	2.505	2.979
$\mathbf{2}_{peq}$	MM2(91)	129	133			1.395	3.236	2.214
$\mathbf{3}_{pax}$	MM2(91)	91	99	61	180	1.416	2.498	2.871
$\mathbf{3}_{peq}$	MM2(91)	133	145	62	180	1.416	3.336	2.278
$\mathbf{4}_{pax}$	MM2(91)	89	97	62	180	1.417	2.480	2.919
$\mathbf{4}_{peq}$	MM2(91)	133	144	61	180	1.418	3.334	2.280
$\mathbf{5}_{pax}$	MM2(91)	88	93			1.414	2.389	
$\mathbf{5}_{peq}$	MM2(91)	133	142			1.416	3.302	
$\mathbf{6}_{peq}$[b]	MM2(91)	131	146			1.419	3.323	2.276
	X-ray	128	132			1.440	3.218	2.169

[a] MM2(91), see refs 16 and 17; the default value (1.5) was used for the dielectric constant. [b] Energy minimization of **6** gave $\mathbf{6}_{peq}$ both with a pax and peq starting conformation.

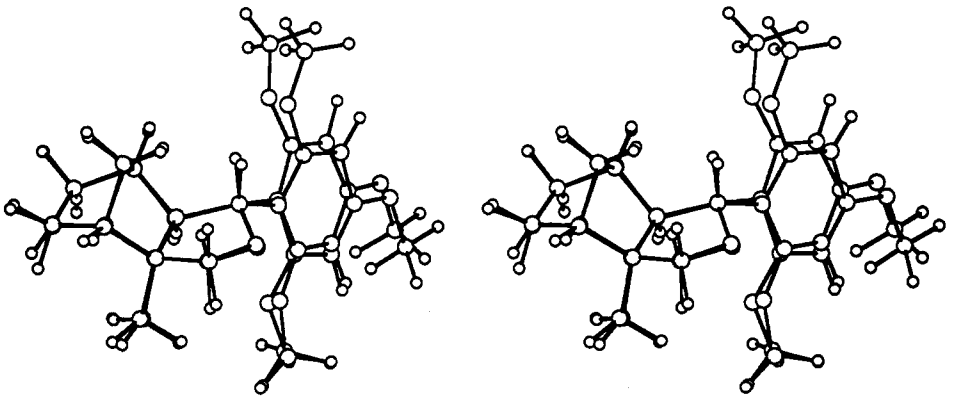

Figure 7. Stereoview of the superimposed X-ray and MM2(91) structures of $\mathbf{6}_{peq}$, obtained by least-squares fitting of carbon and oxygen atoms 1–10.

Table 4. Conformational Energies and Calculated and Experimental Coupling Constants (J_{H5-H6}) for Compounds **1–8**

compd	energy[a] (kJ/mol)	Boltzman distribution[b]	J_{H5-H6} (Hz); Karplus[c]	J_{H5-H6} (Hz); exptl[d]
$\mathbf{1}_{pax}$	0.0	99	~0	0.0
$\mathbf{1}_{peq}$	10.0	1		
$\mathbf{2}_{pax}$	0.0	99	~0	0.0
$\mathbf{2}_{peq}$	10.6	1		
$\mathbf{3}_{pax}$	6.0	8	~6	6.3
$\mathbf{3}_{peq}$	0.0	92		
$\mathbf{4}_{pax}$	4.5	14	~6	7.9
$\mathbf{4}_{peq}$	0.0	86		
$\mathbf{5}_{pax}$	0.0	56	~2	4.8[e]
$\mathbf{5}_{peq}$	0.6	44		
$\mathbf{6}_{peq}$	*f*	100	~7	7.6
7	*g*	*g*	*g*	1.4
8	*g*	*g*	*g*	4.0

[a] Calculated for the global minimum conformations, using the MacMimic/MM2(91) package.[16,17] The lowest energy for a pax/peq pair was set to 0.0. [b] Calculated using the expression $N_{pax}/N_{peq} = \exp -[(E_{pax} - E_{peq})/k^*T]$ for the global minimum energies. [c] Determined from the Karplus curves[15] and weighted by the Bolzman distribution. [d] Determined at 500 MHz with a Bruker ARX500 instrument. [e] $J_{H5-H6-trans}$. [f] Using $\mathbf{6}_{pax}$ as the starting conformation in the MM2(91) calculation gave $\mathbf{6}_{peq}$ as the final conformation. [g] The sulfur and nitrogen parameters used in the MM2(91) program give no meaningful data for **7** and **8**.

distance is intermediate between that of the pax and peq conformations. However, the carbonyl group of **9** seems to reduce the electron density on O_4, resulting in a less pronounced deshielding/shielding of H_{10a}/H_{10b} (Table 1).

The strong oxygen-induced deshielding in the compounds that prefer a peq conformation (**3**, **4**, and **6**) was unexpected. Therefore, it seems pertinent to modify the van der Waals contact requirement[18,19] for cases like those presented here, where the deshielded hydrogen lies in the plane defined by the oxygen atom and its lone pairs of electrons. Put another way, in this plane, the effective deshielding range of oxygen may exceed that of its normal van der Waals radius. However, being of substantial general interest, the problem requires additional experimental and theoretical attention.

Conclusions

Conformationally restricted *O*- and *S*-furanosides, where the ring carbons are kept in one plane, allowing only the ring oxygen to move above or below the plane, preferred the conformation with a pseudoaxial anomeric substituent. The corresponding *C*-furanosides instead preferred the conformation with a pseudoequatorial substituent. These findings constitute experimental evidence of an anomeric effect in furanosides.

Experimental Section

Melting points are uncorrected. Optical rotations were measured with a Perkin-Elmer 141 polarimeter. ^{1}H-NMR spectra were recorded with a Varian XL-300 and a Bruker ARX-500 instrument. Chemical shifts are given in ppm downfield from the signal for Me_4Si, with reference to internal $CHCl_3$ (7.26 ppm), as shown in Table 1. Thin layer chromatography was performed on Kiselgel 60 F254 plates (Merck). Column chromatography was performed on SiO_2 (Matrex LC-gel; 60A, 35-70 MY, Grace). HPLC purifications were performed using an Apex Prepsil ODS (8 μm) column, a Beckman 110B Solvent Delivery Module, a LDC UVIII Monitor (254 nm), and a NEC PC-8300 control unit.

Molecular Mechanics. MM2 calculations were performed with the MacMimic/MM2(91) package[17] using standard parameters only. The MM2(91) program was the unadulterated version developed by Allinger and co-workers.[16,20] The standard force field includes treatment of the O–C–O anomeric effect as described in ref 20.

(–)-(1*S*,2*S*,5*R*,6*R*,7*S*)-2-Methyl-5-(benzyloxy)-4-oxatricyclo[5.2.1.0^{2,6}]-decane (1). To a solution of the aldehyde **11** (1.605 g, 5.89 mmol) in diethylene glycol (10 mL) were added KOH (1.22 g, 21.8 mmol) and hydrazine hydrate (890 μL, 18.3 mmol). The mixture was heated to 130 °C, and the water was distilled off. The temperature was then gradually

(20) Norskov-Lauritsen, L.; Allinger, N. L. *J. Comput. Chem.* **1984**, *5*, 326.

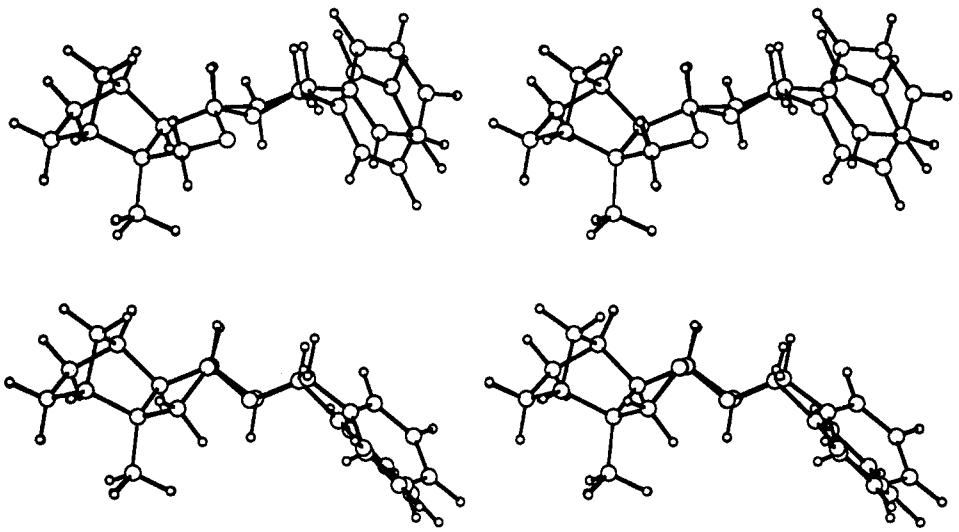

Figure 8. Stereoview of the superimposed energy-minimized (MM2) $\mathbf{1}_{pax}/\mathbf{4}_{pax}$ and $\mathbf{1}_{peq}/\mathbf{4}_{peq}$ conformations, obtained by least-squares fitting of carbon and oxygen atoms 1–10.

raised during 30 min to 200 °C. After another 30 min, the mixture was cooled to room temperature and water (50 mL) was added. After extraction with diethyl ether (6 × 20 mL), the organic phase was dried (Na_2SO_4) and concentrated. Column chromatography (heptane/EtOAc 4:1) gave **1** (1.32 g, 87%). Compound **1** was further purified by HPLC (MeOH/water 1:1 → MeOH): $[\alpha]_D^{20}$ −120.2° (*c* 1.5, $CHCl_3$); ^{1}H-NMR ($CDCl_3$) δ 7.35 (s, 5 H, ArH) and Table 1; MS *m/z* calcd for $C_{17}H_{22}O_2$ (M + 1) 259.1698, found 259.1695.

(−)-(1*S*,2*S*,5*R*,6*R*,7*S*)-2-Methyl-5-hydroxy-4-oxatricyclo[5.2.1.0^{2,6}]decane (2). To a solution of **1** (461 mg, 1.785 mmol) in tetrahydrofuran (35 mL) was added Pd/C (10%, 900 mg) under nitrogen. Hydrogenation (H_2, 1 atm) for 24 h followed by filtration (Celite), concentration, and column chromatography (heptane/EtOAc 4:1) gave **2** and its anomer **2**α (262 mg, 88%, β/α 97:3). Further chromatography gave pure **2**: $[\alpha]_D^{20}$ = −72.2° (*c* 1.4, $CHCl_3$); ^{1}H-NMR ($CDCl_3$) δ 2.30 (d, 1 H, *J* = 2.5 Hz, OH) and Table 1.

(+)-(1*S*,2*S*,5*S*,6*R*,7*S*)-2-Methyl-5-(2-oxo-2-phenylethyl)-4-oxatricyclo[5.2.1.0^{2,6}]decane (3). 1-Phenyl-2-((trimethylsilyl)oxy)ethylene (135 μL, 0.66 mmol) and boron trifluoride etherate (120 μL, 0.88 mmol) were added to a solution of **1** (114 mg, 0.44 mmol) in dichloromethane (9 mL). The mixture was stirred for 10 min, and saturated aqueous $NaHCO_3$ was added. The mixture was extracted with dichloromethane, and the extract was washed with water, concentrated, and dried (Na_2SO_4). The residue was chromatographed (SiO_2, heptane/EtOAc 20:1) to give **3** (115 mg, 97%). Compound **3** was further purified by HPLC (MeOH/water 1:1 → MeOH): $[\alpha]_D^{20}$ +3.1° (*c* 1.3, $CHCl_3$); ^{1}H-NMR ($CDCl_3$) δ 7.4–8.0 (m, 5 H, ArH) and Table 1; MS *m/z* calcd for $C_{18}H_{22}O_2$ (M) 270.1620, found 270.1632.

(−)-(1*S*,2*S*,5*S*,6*R*,7*S*)-2-Methyl-5-(2-phenylethyl)-4-oxatricyclo[5.2.1.0^{2,6}]decane (4). KOH (46 mg, 0.82 mmol) and hydrazine hydrate (33 μL, 0.68 mmol) were added to a solution of **3** (60 mg, 0.22 mmol) in diethylene glycol (0.45 mL). The mixture was heated at 120 °C for 30 min. Water was removed, and the mixture was gradually heated to 200 °C during 30 min and then kept at 200 °C for another 30 min. The mixture was cooled to room temperature, and water (1 mL) was added. The mixture was extracted with dichloromethane, concentrated, and dried (Na_2SO_4). The residue was chromatographed (SiO_2, heptane/EtOAc 20:1 → 10:1) to give **4** (28 mg, 51%). Compound **4** was further purified by HPLC (MeOH/water 1:1 → MeOH): $[\alpha]_D^{20}$ −20.1° (*c* 1.3, $CHCl_3$); ^{1}H-NMR ($CDCl_3$) δ 7.1–7.3 (m, 5 H, ArH) and Table 1; MS *m/z* calcd for $C_{18}H_{24}O$ (M) 256.1827, found 256.1829.

(1*S*,2*R*,6*R*,7*S*)-2-Methyl-4-oxatricyclo[5.2.1.0^{2,6}]decane (5). The diol **12** (57 mg, 0.33 mmol) was added to a solution of triphenylphosphine (96 mg, 0.37 mmol) in deuteriochloroform (2.4 mL), then diethyl azodicarboxylate (DEAD, 64 μL, 0.37 mmol) was added under a constant flow of nitrogen. After the mixture was refluxed for 2 h, diethyl ether (7 mL) was added. The ether phase was washed with hydrochloric acid (2 M, 4 mL) and saturated aqueous $NaHCO_3$. The water phase was extracted with diethyl ether, the combined organic phase was dried (Na_2SO_4), and the ether was distilled off. The residue was chromatographed (diethyl ether/pentane 1:10). The pure fractions were concentrated and deuteriochloroform (3 mL) was added and partly removed: ^{1}H NMR see Table 1; MS *m/z* calcd for $C_{10}H_{16}O$ (M + 1) 153.1279, found 153.1279.

(+)-(1*S*,2*S*,5*R*,6*R*,7*S*)-2-Methyl-5-(2,4,6-trimethoxyphenyl)-4-oxatricyclo[5.2.1.0^{2,6}]decane (6). To a solution of **1** (59 mg, 0.23 mmol) in dichloromethane (4.5 mL) were added 1,3,5-trimethoxybenzene (60 mg, 0.35 mmol) and boron trifluoride etherate (60 μL, 0.47 mmol). After 10 min, aqueous HCl (20 mL, 2 M) was added. The mixture was extracted with diethyl ether three times, and the extract was dried (Na_2SO_4) and concentrated. The residue was chromatographed (heptane/EtOAc 4:1) to give **6** (67 mg, 93%). An analytical sample was recrystallized from heptane: $[\alpha]_D^{20}$ +17.6° (*c* 1.0, $CHCl_3$); mp 114.5–115.0 °C; ^{1}H-NMR ($CDCl_3$) δ 6.11 (s, 2 H, ArH), 3.80 (s, 3 H, OMe), 3.79 (s, 6 H, OMe) and Table 1; MS *m/z* calcd for $C_{19}H_{26}O_4$ (M + 1) 319.1909, found 319.1905. Anal. Calcd for $C_{19}H_{26}O_4$: C, 71.7; H, 8.2. Found: C, 71.7; H, 7.9.

(−)-(1*S*,2*S*,5*R*,6*R*,7*S*)-2-Methyl-5-(benzylthio)-4-oxatricyclo[5.2.1.0^{2,6}]decane (7). To a solution of **1** (57 mg, 0.22 mmol) in dichloromethane (4 mL) was added benzyl mercaptan (65 μL, 0.55 mmol) and boron trifluoride etherate (55 μL, 0.44 mmol). The mixture was stirred for 10 min, and triethylamine (2 mL) was added. The mixture was concentrated and the residue chromatographed (heptane/EtOAc 20:1) to give **7** (59 mg, 97%). The compound was further purified by HPLC (MeOH/water 1:1 → MeOH): $[\alpha]_D^{20}$ −270° (*c* 1.4, $CHCl_3$); ^{1}H-NMR ($CDCl_3$) δ 7.3–7.4 (m, 5H, ArH) and Table 1; MS *m/z* calcd for $C_{17}H_{22}OS$ (M + 1) 275.1470, found 275.1476.

(+)-(1*S*,2*S*,5*S*,6*R*,7*S*)-2-Methyl-5-(1-*N*-thyminyl)-4-oxatricyclo[5.2.1.0^{2,6}]decane (8). Thymine (60 mg, 0.48 mmol) was dissolved in hexamethyldisilazane (840 μL), and trimethylchlorosilane (84 μL) was added. The solution was heated to 140 °C, dimethylformamide (10 μL) was added, and the mixture was refluxed until a clear solution was obtained. The solution was cooled to room temperature and concentrated. The residue was dissolved in dichloromethane (2.2 mL) and added to **7** (60 mg, 0.22 mmol). A molecular sieve (4 Å, 150 mg) was added, the mixture was cooled to −70 °C and *N*-bromosuccinimide (40 mg) was added. The mixture was stirred for 1.5 h. Aqueous $Na_2S_2O_3$ (1 M, 4 mL) was added, and the mixture was extracted with dichloromethane and dried (Na_2SO_4). The organic phase was concentrated and the residue chromatographed (heptane/EtOAc 2:1) to give **8** and **13** (56 mg, 0.20 mmol, 92%) as a diastereomeric mixture. The isomers were partially separated by column chromatography (*tert*-butyl methyl ether/toluene/diethylamine 10:10:1) to give 10 mg of each isomer. These were further purified by HPLC (MeOH/water 1:1 → MeOH). Compound **8**: $[\alpha]_D^{20}$ +20.3° (*c* 0.9, $CHCl_3$); ^{1}H-NMR ($CDCl_3$) δ 8.72 (s, 1 H, NH), 7.13 (q, 1 H, *J* = 1.2 Hz, thymineH), 1.94 (d, 3 H, *J* = 1.2 Hz, thymineMe) and Table 1; MS *m/z* calcd for $C_{15}H_{20}N_2O_3$ (M + 1) 277.1552, found 277.1549.

(−)-(1*S*,2*S*,6*R*,7*S*)-2-Methyl-4-oxa-5-oxotricyclo[5.2.1.0^{2,6}]decane (9). To a solution of CrO_3 (922 mg, 9.22 mmol) and pyridine (1.45 mL) in dichloromethane (23 mL) was added a solution of the hemiacetal **2** (220 mg, 1.315 mmol) in dichloromethane (10 mL). After 20 min, the mixture was washed with aqueous NaOH (5%), aqueous HCl (1 M) and saturated

aqueous $NaHCO_3$. The organic phase was dried (Na_2SO_4) and concentrated. Column chromatography (heptane/EtOAc 4:1) gave **9** (154 mg, 70%): $[\alpha]_D^{20}$ −35.4° (*c* 0.8, $CHCl_3$); ^{1}H-NMR see Table 1; MS *m/z* calcd for $C_{10}H_{14}O_2$ (M + 1) 167.1072, found 167.1073.

(−)-(1*S*,2*R*,5*R*,6*R*,7*S*)-2-Formyl-5-(benzyloxy)-4-oxatricyclo[5.2.1.0^{2,6}]-decane (11). The aldehyde **10**[20] (2.631 g, 9.73 mmol) was dissolved in sodium methoxide/methanol (260 mL, 0.03 M), and Pd/C (10%, 420 mg) was added under nitrogen. After hydrogenation (1 atm) for 40 min, the mixture was filtered (Celite) and concentrated. Column chromatography (heptane/EtOAc 10:1) gave **11** (1.767 g, 67%): $[\alpha]_D^{20}$ −117.1° (*c* 1.4, $CHCl_3$); ^{1}H-NMR ($CDCl_3$) δ 9.83 (s, 1 H, CHO), 7.32 (s, 5H, ArH) and Table 1.

(+)-(1*R*,2*S*,3*R*,4*S*)-2-Methyl-2,3-bis(hydroxymethyl)bicyclo[2.2.1]-heptane (12). The hemiacetal **2** (50 mg, 0.30 mmol) was dissolved in diethyl ether (1.7 mL), and lithium aluminum hydride (17 mg, 0.45 mmol) was added. The mixture was stirred for 6 min. Saturated aqueous K_2CO_3 (0.1 mL) and water (2 mL) were carefully added, and the solution was extracted with dichloromethane (3 mL). The organic phase was washed with water three times. The water phase was extracted with dichloromethane. The combined organic phase was dried (Na_2SO_4) and concentrated. Filtration on SiO_2 with ethyl acetate gave **12** (47 mg, 92%): $[\alpha]_D^{20}$ +19.4° (*c* 0.6, $CHCl_3$); ^{1}H-NMR see Table 1; MS *m/z* calcd for $C_{10}H_{18}O_2$ (M + 1) 171.1385, found 171.1385.

(−)-(1*S*,2*S*,5*R*,6*R*,7*S*)-2-Methyl-5-(1-*N*-thyminyl)-4-oxatricyclo-[5.2.1.0^{2,6}]decane (13). Compound **13** was isolated as described in the preparation of **8**. Compound **13**: $[\alpha]_D^{20}$ −95.6° (*c* 0.8, $CHCl_3$); ^{1}H-NMR ($CDCl_3$) δ 8.63 (s, 1 H, NH), 7.41 (d, 1 H, *J* = 1.2 Hz, thymineH), 1.93 (d, 3 H, *J* = 1.2 Hz, thymine Me) and Table 1; MS *m/z* calcd for $C_{15}H_{20}N_2O_3$ (M + 1) 277.1552, found 277.1556.

Acknowledgments. We are grateful to Dr. John F. Richardson, College of Arts and Sciences, University of Louisville, Kentucky, for the X-ray crystal analysis. This work was supported by The Swedish Natural Science Research Council.